Magnetization jump in the XXZ chain with next-nearest-neighbor exchange

A. A. Aligia
Comisión Nacional de Energía Atómica, Centro Atómico Bariloche and Instituto Balseiro, 8400 S.C. de Bariloche, Argentina
(Received 29 June 2000; revised manuscript received 8 September 2000; published 11 December 2000)

We study the dependence of the magnetization M with magnetic field B at zero temperature in the spin-1/2 XXZ chain with nearest-neighbor (NN) J_1 and next-NN J_2 exchange interactions, with anisotropies Δ_1 and Δ_2, respectively. The region of parameters for which a jump in $M(B)$ exists is studied using numerical diagonalization, and analytical results for two magnons on a ferromagnetic background in the thermodynamic limit. We find a line in the parameter space $(J_2/J_1, \Delta_1/J_1, \Delta_2/J_1)$ (determined by two simple equations) at which the ground state is highly degenerate. $M(B)$ has a jump near this line, and at or near the isotropic case with ferromagnetic J_1 and antiferromagnetic J_2, with $|J_2/J_1| \sim 1/4$. These results are relevant for some systems containing CuO chains with edge-sharing CuO_4 units.

DOI: 10.1103/PhysRevB.63.014402 PACS number(s): 75.10.Jm, 75.30.Kz

I. INTRODUCTION

In recent years quantum spin chains and ladders have been a subject of great experimental and theoretical interest. Quasi-one-dimensional magnetic systems have been identified and studied experimentally,[1–4] and new theoretical studies of the spin-1/2 XXZ chain with nearest-neighbor (NN) and next-NN exchange coupling (which is equivalent to a two-leg zig-zag ladder) were presented.[4–14] The Hamiltonian is

$$H=\sum_i [J_1(S_i^x S_{i+1}^x + S_i^y S_{i+1}^y + \Delta_1 S_i^z S_{i+1}^z) + J_2(S_i^x S_{i+2}^x + S_i^y S_{i+2}^y + \Delta_2 S_i^z S_{i+2}^z)]. \quad (1)$$

One of the properties of this model is that the magnetization as a function of applied magnetic field $M(B)$ displays a jump for certain parameters.[9,11] This phenomenon called metamagnetic transition was observed for example in TmSe,[15] $Fe_xMn_{1-x}TiO_3$,[16] $Tb_{1-x}Sc_xMn_2$,[17] and the quasi-one-dimensional compound $Ba_3Cu_2O_4Cl_2$.[18]

Previous studies of metamagnetism in the model were restricted to $\Delta_1=\Delta_2=\Delta$.[9,11] The results show that a jump in $M(B)$ is not possible if $\Delta>\Delta_c$. Following the methods explained in Sec. III, we have determined $\Delta_c=(-5+\sqrt{17})/4 \cong -0.22$.[19] In principle, the requirement of an opposite sign for the z component of the exchange rather than for the other two seems unrealistic. However, for the Hamiltonian, Eq. (1), a negative Δ_1 with positive J_1 is equivalent to a positive Δ_1 with negative J_1, since a rotation of every second spin in π around the z axis changes the sign of the x and y components of J_1. Thus, $\Delta_1<\Delta_c$ does not necessarily mean a large anisotropy of Δ_1. Instead, a negative $\Delta_2<\Delta_c$ is a very large anisotropy of J_2 and seems difficult to find in real systems.

In this paper we extend the previous searches of metamagnetic transitions to arbitrary values of Δ_1 and Δ_2, concentrating our study in $|\Delta_1| \leqslant 1$ and $0 \leqslant \Delta_2 \leqslant 1$, and particularly near the isotropic case of ferromagnetic J_1 and antiferromagnetic J_2. Several systems containing CuO chains with edge-sharing CuO_4 units, like $La_6Ca_8Cu_{24}O_{41}$, Li_2CuO_2, and $Ca_2Y_2Cu_5O_{10}$, are expected to lie near this limit.[20] In these systems, the Cu-O-Cu angle θ of the CuO chains is near 90° and therefore, the usual antiferromagnetic NN exchange is largely frustrated. As a consequence of virtual processes in which the Hund rules exchange integral at the O atoms play a role, J_1 becomes small and ferromagnetic. We estimate the critical field B_c at which a jump or an abrupt increase in $M(B)$ should exist in these compounds.

The outline of the paper is as follows. In Sec. II we explain how we determine the regions of parameters for which a metamagnetic transition is expected. Section III contains analytical results for the onset of bound states of two magnons in a ferromagnetic background. These results and numerical ones in chains of 20 sites are used in Sec. IV to present phase diagrams in which the boundaries of the metamagnetic regions are shown. This section includes numerical results for the ground-state energy per site as a function of magnetic field $E(M)$, curves of $M(B)$, and critical field B_c as a function of $\alpha=J_2/J_1$ for $\Delta_2=-\Delta_1=1$. Section V contains a more detailed numerical study of this isotropic case for α slightly larger than 1/4. Section VI is a summary and discussion.

II. CONDITIONS FOR THE EXISTENCE OF A JUMP IN $M(B)$

For the sake of clarity, we anticipate some of our numerical results for the dependence of the ground-state energy per site E as a function of magnetization $M=S^z/L$, where $S^z=\Sigma_i S_i^z$ is the z component of the total spin and L is the number of sites. They are shown in Fig. 1. A large portion of the curve $E(M)$ has negative curvature. These points are actually not accessible thermodynamically. The dashed straight line is tangent to $E(M)$ at the two points $M_1=0.108$ and $M_2=0.5$ (the Maxwell construction). For all M in the interval (M_1,M_2), it is energetically more favorable for the system to phase separate into a fraction $x=(M-M_1)/(M_2-M_1)$ with magnetization M_2 and a fraction $1-x$ with magnetization M_1. The energy of the mixture is represented by the dashed line. If a magnetic field B is applied to the system, the equilibrium magnetization is deter-

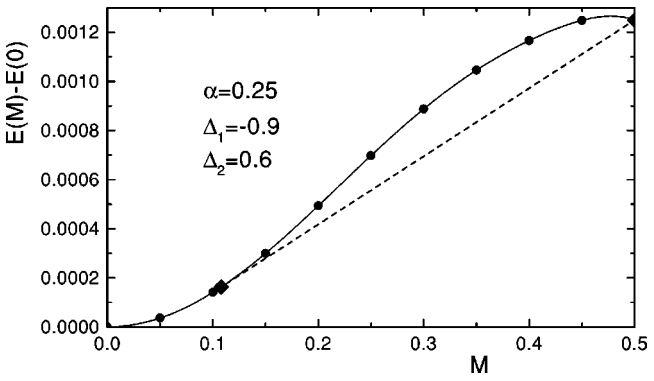

FIG. 1. Energy per site as a function of total z component of spin per site for a chain of 20 sites (solid circles). The full line is a polynomial fit. Dashed line and diamonds correspond to the Maxwell construction. Parameters are $J_1=1$, $\alpha=J_2/J_1=0.25$, $\Delta_1=-0.9$, and $\Delta_2=0.6$.

mined minimizing the Helmholz transform $G=E-MB$, what leads to the condition $B=\partial E/\partial M$. From inspection of Fig. 1, we see that $M(B)$ increases with B, until it reaches the critical value $B_c=[E(M_2)-E(M_1)]/(M_2-M_1)$ $(=0.002\,77J_1$ for the case of Fig. 1). At $B=B_c$, $M(B)$ suddenly jumps from M_1 to M_2. If M_2 is smaller than the saturation magnetization, M increases further for $B>B_c$, but we have not found this situation in the present model.

From the above description, one can see that for a metamagnetic transition to occur at very low temperatures, $E(M)$ should satisfy two conditions: (1) $\partial^2E/\partial M^2<0$ in a finite interval of values of M. (2) $E(M_2)>E(M_1)$, where $M_1<M_2$ are determined by the Maxwell construction. From the general behavior of $E(M)$ for the case $\Delta_1=\Delta_2=\Delta$, Gerhardt *et al.*[9] have found that when metamagnetism exists, $M_2=1/2$ and the condition 2 ceases to be satisfied when $M_1=0$. More precisely, from their finite-size results for $E(M,\alpha,\Delta)$, with $\alpha=J_2/J_1$, they obtained a critical value of Δ $[\Delta^f(\alpha)]$ from the equation $E(0,\alpha,\Delta^f)=E(1/2,\alpha,\Delta^f)$. For $\Delta<\Delta^f$ the system is a fully spin-polarized ferromagnet even at $B=0$. Fortunately, the results for Δ^f do not show a significant size dependence and it is accurately determined in chains of 18 sites. Another critical value $\Delta^a(\alpha)$ was obtained from the condition $\partial^2E/\partial M^2|_{M=1/2}=0$. For $\Delta>\Delta^a$ the curvature $\partial^2E/\partial M^2$ is positive for all M. The curvature at M_2 was calculated numerically using

$$\partial^2E/\partial M^2|_{M=1/2}=\lim_{L\to\infty}L^2[E(1/2)+E(1/2-2/L)-2E(1/2-1/L)] \tag{2}$$

in a periodic chain. In contrast to the case of Δ^f, and even taking $L=50$, the result has some finite-size effects.[9] This is in part due to the fact (explained in the next section) that the ground state near $M=1/2$ becomes incommensurate for sufficiently large α, and these wave vectors cannot be represented in small chains if periodic boundary conditions are used.[12] From the numerical solution of the problem of two spin excitations on the ferromagnetic state for $L\to\infty$, more accurate values of $\Delta^a(\alpha)$ were obtained recently for $\alpha\leqslant 1/2$.[11] In the region of the (α,Δ) plane, where $\Delta^f(\alpha)<\Delta<\Delta^a(\alpha)$ a metamagnetic transition occurs in the model.[9,11]

Relaxing the condition $\Delta_1=\Delta_2=\Delta$, and keeping, for example, Δ_2 fixed, limiting values of Δ_1 $[\Delta_1^f(\alpha,\Delta_2)$ and $\Delta_1^a(\alpha,\Delta_2)]$ can be defined in the same way and we expect in principle that magnetization jumps will be found if $\Delta_1^f(\alpha,\Delta_2)<\Delta_1<\Delta_1^a(\alpha,\Delta_2)$. The same is true interchanging Δ_1 and Δ_2. Fortunately, as described in the next section, the Δ_i^a are given by analytical expressions, which are very simple near $\alpha=1/4$. The Δ_i^f are determined by numerical diagonalization of chains with $L=20$ and the results are given in Sec. IV.

III. THE TWO-MAGNON PROBLEM

In this section, we derive analytical expressions for the upper boundaries of the expected metamagnetic region $[\Delta_1^a(\alpha,\Delta_2)$ or $\Delta_2^a(\alpha,\Delta_1)]$, looking for bound states of two spin flips on a ferromagnetic background in an infinite chain. This is a two-body problem, which due to translational invariance can be mapped into a single-body one. Similar problems were solved for example, to determine exactly metal-insulator boundaries in generalized Hubbard models.[21] For $\Delta_1=\Delta_2=\Delta$, this problem has been solved numerically for $L\sim 150$ by Cabra *et al.*[8] and for $L\to\infty$ and $\alpha\leqslant 1/2$ by Hirata.[11] Simple analytical expressions are given in Ref. 19.

We use a Jordan-Wigner transformation $S_j^+=c_j^\dagger\exp(i\pi\Sigma_{l<j}n_l)$, $S_j^-=(S_j^+)^\dagger$, $S_j^z=n_j-1$, with $n_j=c_j^\dagger c_j$, to express the spin operators in terms of spinless fermions. Calling $\alpha=J_2/J_1$, setting $J_1=1$ as the unit of energy, and substracting the constant $LE(1/2)$ [with $E(1/2)=(\Delta_1+\alpha\Delta_2)/4$], the Hamiltonian equation (1) takes the form

$$H=\sum_i\ [(-\Delta_1-\alpha\Delta_2)n_i+\tfrac{1}{2}(c_{i+1}^\dagger c_i+\alpha c_{i+2}^\dagger c_i+\text{H.c.}) +\Delta_1 n_i n_{i+1}+\alpha\Delta_2 n_i n_{i+2}-\alpha(c_{i+2}^\dagger n_{i+1}c_i+\text{H.c.})]. \tag{3}$$

After Fourier transform $c_j=\sqrt{1/L}\Sigma_q e^{iqj}c_q$, the model can be written as

$$H=\sum_q\ \epsilon_q c_q^\dagger c_q+\frac{4}{L}\sum_K\ \sum_{q,q'>0}\ [(\Delta_1+2\alpha\cos K)\sin q\sin q' +\alpha\Delta_2\sin 2q\sin 2q']c_{K/2-q'}^\dagger c_{K/2+q'}^\dagger c_{K/2+q}c_{K/2-q}, \tag{4}$$

with $\epsilon_q=-\Delta_1-\alpha\Delta_2+\cos q+\alpha\cos 2q$.

The two-magnon eigenstates of total momentum K can be written in the form $|\psi(K)\rangle=\Sigma_{q>0}A_q c_{K/2-q}^\dagger c_{K/2+q}^\dagger|0\rangle$. Replacing this into the Schrödinger equation $H|\psi\rangle=\lambda|\psi\rangle$, one obtains

$$A_q=\frac{-4[(\Delta_1+2\alpha\cos K)S_1(K)\sin q+\alpha\Delta_2 S_2(K)\sin 2q]}{\epsilon_{K/2-q}+\epsilon_{K/2+q}-\lambda}, \tag{5}$$

where

$$S_n(K)=\frac{1}{L}\sum_{q>0}A_q\sin nq. \tag{6}$$

Replacing Eq. (5) into Eq. (6) leads to two homogeneous equations for the two unknown sums S_1 and S_2. For fixed values of the parameters and K, the condition of vanishing secular determinant determines the allowed eigenvalues λ. Since we are looking for the condition on the parameters for the onset of a bound state [when the right-hand side of Eq. (2) becomes negative], we set λ slightly below two times the minimum one-magnon energy: $\lambda=2\ \min(\epsilon_q)-\eta$, where η is a positive infinitesimal energy. With this value of λ, the condition of vanishing secular determinant in the thermodynamic limit $L\to\infty$ takes the form

$$4(\Delta_1+2\alpha\cos K)[I_0+16\alpha\Delta_2(I_0I_2-I_1^2)]+16\alpha\Delta_2I_2+1=0, \tag{7}$$

where the integrals $I_n(\alpha,K)$ $(n=0,1,2)$ are

$$I_n=\frac{1}{2\pi}\int_0^\pi\frac{dq\,\sin^2q\cos^nq}{4\alpha\cos K\cos^2q+2\cos(K/2)\cos q+c(\alpha,K)+\eta}, \tag{8}$$

with $\eta\to0$ and

$$c(\alpha,K)=2(1-\alpha-\alpha\cos K),\quad \alpha\leqslant1/4,$$

$$c(\alpha,K)=2\alpha+\frac{1}{4\alpha}-2\alpha\cos K,\quad \alpha\geqslant1/4. \tag{9}$$

The change of the expression for $c(\alpha,K)$ at $\alpha=1/4$ is due to the change in the wave vector, which minimizes ϵ_q from $q=\pi$ for $\alpha\leqslant1/4$ to $q=\pm\arccos[-1/(4\alpha)]$ for $\alpha\geqslant1/4$. The integrals can be solved decomposing the integrand into a sum of expressions with denominators linear in $\cos q$ and using[22]

$$\frac{1}{2\pi}\int_0^\pi\frac{dq\,\sin^2q}{a+b\cos q}=\frac{a}{2b^2}\left(1-\sqrt{1-\frac{b^2}{a^2}}\right). \tag{10}$$

For each value of α, K, and Δ_1, Eq. (7) is a linear equation in Δ_2. The searched upper boundary $\Delta_2^a(\alpha,\Delta_1)$ is determined choosing the value of K that leads to the highest root of Eq. (7). For $\Delta_2<\Delta_2^a(\alpha,\Delta_1)$, the curvature equation (2) is negative. The same is true interchanging Δ_1 and Δ_2. If $\Delta_1=\Delta_2=\Delta$ is taken,[9,11] the highest root of the quadratic equation (7) determines $\Delta^a(\alpha)$, since there is at least one bound state for $\Delta<\Delta^a(\alpha)$.

For $\alpha\leqslant1/4$, the total wave vector K, which first leads to a bound state, is $K=0$. In the sector of two particles, this is also the wave vector of the ground state of the noninteracting part of the Hamiltonian in the fermionic representation [Eq. (3) or (4)]. Using Eqs. (8), (9), and (10), we obtain after some algebra

$$I_0=\frac{r-1}{8\alpha},\quad I_1=\frac{1-(1-2\alpha)r}{16\alpha^2},$$

$$I_2=\frac{\alpha-1}{16\alpha^2}+\left(\frac{1}{2\alpha}-1\right)^2I_0,$$

$$\text{with}\quad r=(1-4\alpha)^{-1/2}\quad(\alpha<1/4). \tag{11}$$

Equations (7) and (11) define $\Delta_2^a(\alpha,\Delta_1)$ and $\Delta_1^a(\alpha,\Delta_2)$ for $\alpha<1/4$.

For $\alpha>1/4$, the ground state of the noninteracting fermionic Hamiltonian for two particles is degenerate with total wave vector $K=0$ or $K=\pm K_i$ with $K_i=2\arccos[-1/(4\alpha)]$. For $\Delta_1=\Delta_2$, we have found that the wave vector of the ground state of the two-magnon problem for parameters near the onset of a bound state is $K=0$ for $\alpha\leqslant1/2$. At $\alpha=1/2$ it jumps to $\pm K_i$. From numerical investigations in finite systems (with $L\sim20$), using twisted boundary conditions to allow all possible wave vectors,[12] we find that for values of $\alpha>\alpha_w\sim1$, the ground-state wave vector deviates continuously from $\pm K_i$. Comparison of the numerical results for $\Delta^a(\alpha)$ (with $L\sim50$) of Ref. 9 with our analytical ones assuming $K=\pm K_i$, gives $\alpha_w\cong0.77$. In the region $\alpha>\alpha_w$, it seems not possible to find analytical results for $\Delta^a(\alpha)$. However, taking $K=K_i$ leads to a reasonable lower bound, since K is not too different from K_i (in any case, as we shall see in Sec. V, Eq. (2) ceases to be valid for $\alpha\geqslant\alpha_w$). In the general case $\Delta_1\neq\Delta_2$, the maximum between the results for Δ_n assuming $K=0$ or $K=K_i$, also gives a lower bound for $\Delta_2^a(\alpha,\Delta_1)$ and $\Delta_1^a(\alpha,\Delta_2)$. We restrict the calculation to these values of K. For $K=0$ and $\alpha\geqslant1/4$, the integrals Eq. (8) diverge for $\eta\to0$, and Eq. (10) has complex coefficients for finite η. The equation for the Δ_n is obtained after a careful limiting procedure of Eq. (7) with adequate choice of the branch of the root in Eq. (10). Physically this means simply to consider values of Δ_n slightly smaller than the critical ones, in such a way that they lead to a finite binding energy η, and then take the limit $\eta\to0$. The final results turn out to be very simple:

$$\frac{\Delta_1\Delta_2+\Delta_1}{2\alpha}+\Delta_2\left(1+\frac{1}{8\alpha^2}\right)+1=0\quad(\alpha\geqslant1/4,\ K=0). \tag{12}$$

As an example, this equation is satisfied for $\alpha=1/4$, $\Delta_1=-0.9$, and $\Delta_2=2/3$. Lowering Δ_2 a little bit, $E(M)$ displays the behavior required for a jump in $M(B)$ (see Fig. 1).

Finally, for $\alpha\geqslant1/4$ and $K=K_i$, the integrals take the form

$$I_0=\frac{1}{8\alpha B}\left(1-\frac{1}{4\alpha\sqrt{A}}\right),\quad I_1=\frac{1}{32(\alpha B)^2}\left(\frac{1}{2\alpha}-\frac{1}{\sqrt{A}}\right),$$

$$I_2=\frac{1}{16\alpha}\left(\frac{1}{A}-\frac{1}{B}+\frac{2\alpha-\sqrt{A}}{2\alpha AB^3}\right),$$

with

$$A=1-\frac{1}{16\alpha^2},\quad B=1-\frac{1}{8\alpha^2}\quad(\alpha\geqslant 1/4,\ K=K_i). \tag{13}$$

It remains to establish when Δ_i^a are determined by Eq. (12), or Eq. (13) and Eq. (7) with $\cos K=1/(8\alpha^2)-1$. Taking for instance Δ_1 fixed, and equating the values of Δ_2 obtained from both expressions, we obtain

$$\alpha=-\frac{1}{4\Delta_1},\quad \Delta_2=-1+2\Delta_1^2\quad(-1\leqslant\Delta_1\leqslant 0). \tag{14}$$

For smaller values of α, $\Delta_2^a(\alpha,\Delta_1)$ is determined by Eq. (12). Similarly, for a given value of Δ_2, Eq. (12) gives $\Delta_1^a(\alpha,\Delta_2)$ if $\alpha\leqslant[(1+\Delta_2)/2]^{-1/2}/4$, while for larger values of α, Eqs. (7) and (13) should be used.

Equation (14) defines a particular line in the parameter space $(\alpha,\Delta_1,\Delta_2)$, which as will be seen in the next section, plays an important role in our paper. From the analytical results of this section, we see that at this line, not only is there a degeneracy in the lowest-lying eigenstates in the two-magnon sector (for $M=1/2-2/L$ with $L\to\infty$) between the wave vectors $K=0$ and $K=\pm K_i$, but also $\lim_{L\to\infty}L[E(1/2-1/L)-E(1/2)]=\epsilon_{\arccos(\Delta_1)}=0$ and $\lim_{L\to\infty}L[E(1/2-2/L)-E(1/2)]=0$. In other words $E(M)$ is independent of M for $M\sim 1/2$ in the thermodynamic limit.

IV. PHASE DIAGRAM FOR METAMAGNETIC TRANSITIONS

In this section, we delimit the region of parameters inside which a jump in the function $M(B)$ is expected. Specifically for each α and Δ_1, we determine by numerical diagonalization of chains of 20 sites the lower boundary Δ_2^f of the metamagnetic region [from $E(1/2)=E(0)$], while the upper boundary Δ_2^a (or a lower bound of it for large α) is taken from the expressions of the previous section. The same is done interchanging Δ_1 and Δ_2. This study is complemented by numerical calculations of the ground-state energy as a function of magnetization $E(M)$ [from which $M(B)$ can be derived], and the critical field B_c for several parameters inside the region of interest.

In Fig. 2 we show Δ_2^f (discrete points) and Δ_2^a (thick curve above it) as a function of α for several values of Δ_1. The region of interest $\Delta_2^f<\Delta_2<\Delta_2^a$ is shown by vertical dashed lines for $\Delta_1=-0.7$. Clearly the upper boundary Δ_2^a displays two kinks as a result of the change in the ground-state wave vector for one magnon at $\alpha=1/4$, or two magnons at $\alpha=-1/(4\Delta_1)$, as described in the previous section. Δ_2^a is given by Eqs. (11) and (7) with $K=0$ for $\alpha<1/4$, by Eq. (12) between both kinks, and (as a lower bound) by Eqs. (13) and (7) with $\cos K=1/(8\alpha^2)-1$ for $\alpha>-1/(4\Delta_1)$, respectively.

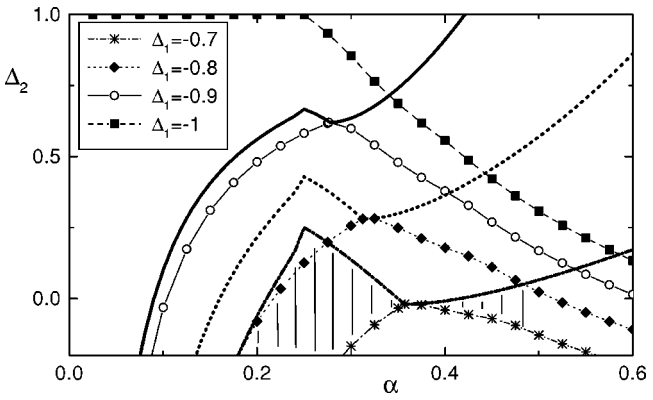

FIG. 2. Boundaries of the region of expected metamagnetic transitions in the (α,Δ_2) plane, for different values of Δ_1. This region is shown dashed for $\Delta_1=-0.7$. The symbols (joined by thin lines) indicate the lower boundary Δ_2^f calculated numerically in chains of 20 sites. The upper boundary Δ_2^a (thick lines) is taken from the analytical results of Sec. III.

It is remarkable that at the second kink [determined by Eqs. (14)], where the wave vector of the two-magnon ground state jumps from $K=0$ to $K=\pm K_i$ and $\partial E/\partial M|_{M=1/2}=\partial^2 E/\partial M^2|_{M=1/2}=0$ for $L\to\infty$ according to the results of the previous section, also $E(1/2)=E(0)$ (at least within the accuracy of the Lanczos diagonalization and independently of system size). Actually $E(M)$ is quite flat at this point. Specifically, we find by numerical diagonalization, that *if and only if* the energy for each value of S^z is minimized with respect to the optimum twisted boundary conditions,[12] $E(M)$ becomes independent of M at this point, within our precision of 10^{-9}. All wave vectors at the minimum become incommensurate except for $S^z=0$ and $S^z=L/2$. For $S^z=L/2-2$, we find that the minimum is at wave vector $K=K_i$, while the energy at $K=0$ is of the order of 10^{-5} above the minimum energy for $L=20$, due to finite-size effects.

Particular cases of degeneracy at the line determined by Eqs. (14) are already known. The degeneracy at the point $\alpha=1/4$, $\Delta_1=-1$, $\Delta_2=1$ was studied by Hamada *et al.*, who also have shown that the ground state in the sector of total spin $S=0$ is a resonance-valence-bond state involving singlet pairs at all distances.[23] The degeneracy at the Majumdar-Ghosh point $\alpha=1/2$, $\Delta_1=\Delta_2=-1/2$, was discussed by Gerhardt *et al.*[9] For $\Delta_1\to 0$, this point moves towards two decoupled ferromagnetic Heisenberg chains [see Eqs. (14)], for which $E(M)$ is constant.

This special point where Δ_2^f and Δ_2^a coincide separates the region of expected metamagnetism in two zones. The one at the left of the point shrinks and moves towards $\Delta_2=1$ as Δ_1 decreases approaching the isotropic limit $\Delta_1=-1$, where it disappears. The right zone also displaces towards $\Delta_2=1$, but increases as Δ_1 moves to -1, suggesting that a jump in $M(B)$ is also possible in the isotropic limit $\Delta_2=-\Delta_1=1$, if $\alpha>1/4$. Figure 3 shows the same two metamagnetic zones in the (α,Δ_1) plane for several values of Δ_2. The same tendencies as before are observed as the isotropic limit $\Delta_2=-\Delta_1=1$ is approached.

In the zone of lower α, the existence of a jump in $M(B)$

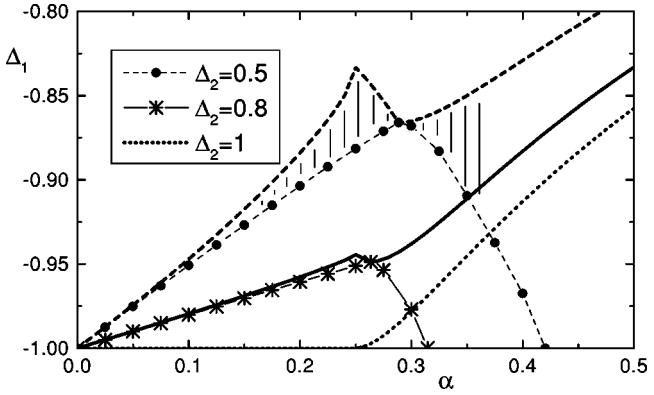

FIG. 3. Boundaries of the region of expected metamagnetic transitions in the (α,Δ_1) plane, for different values of Δ_2. This region is shown dashed for $\Delta_2=0.5$. The symbols (joined by thin lines) indicate the lower boundary Δ_1^f calculated numerically in chains of 20 sites. The upper boundary Δ_1^a (thick lines) is taken from the analytical results of Sec. III.

is confirmed by numerical calculation of $E(M)$. An example was shown in Fig. 1. Instead, inside the right zone of expected metamagnetism (for α larger than the point of degeneracy at which Δ_2^f and Δ_2^a meet), the situation is not so clear. As it is clear in Fig. 4 for $\alpha=1/2$, the energy per site as a function of the z component of the total spin $S^z=\Sigma_i S_i^z = ML$, shows a significant even-odd effect for small chains. This effect has been reduced minimizing $E(M)$ with respect to the optimum twisted boundary conditions to allow for incommensurate wave vectors.[12] Most of the resulting wave vectors are incommensurate, particularly for odd S^z and low $\alpha>1/4$. In spite of this procedure, for $\alpha>0.4$, all $E(M)$ for odd S^z seem to be shifted to higher energies in comparison with the corresponding values for even S^z. If this tendency persists in the thermodynamic limit (keeping L even) states with odd S^z would not be accessible thermodynamically, and the calculation of the previous section [based on Eq. (2)] would be irrelevant. In any case $E(M)$ is very flat for $0.3<M<0.5$ (see Fig. 4) and if the curvature at $M=1/2$ is positive, there would be a steep increase in $M(B)$ for $M>0.3$, which is probably hard to distinguish experimentally from a jump. The determination of the critical value of α for which $\partial^2 E/\partial M^2|_{M=1/2}$ changes sign, is a difficult task which is postponed to the next section.

The continuous curves in Fig. 4 correspond to fits in the numerical data using a polynomial of even powers of M with about half as many parameters as points to be fitted (to average the even-odd effect). These continuous curves allowed us to perform the Maxwell construction analytically (dashed lines and diamonds in Fig. 4), and to calculate $B(M)$ from $B=\partial E/\partial M$ (see Sec. II). The magnetization curve $B(M)$ is shown in Fig. 5 for two values of α, which are near those estimated for $La_6Ca_8Cu_{24}O_{41}$ and $Ca_2Y_2Cu_5O_{10}$, respectively.[20] While the details of the curve and the value of the critical field at the jump B_c (if it exists) depend on the fitting procedure, the fact that there is an abrupt increase from $\sim$60% to 100% of maximum magnetization with a very small variation of magnetic field is a genuine feature of

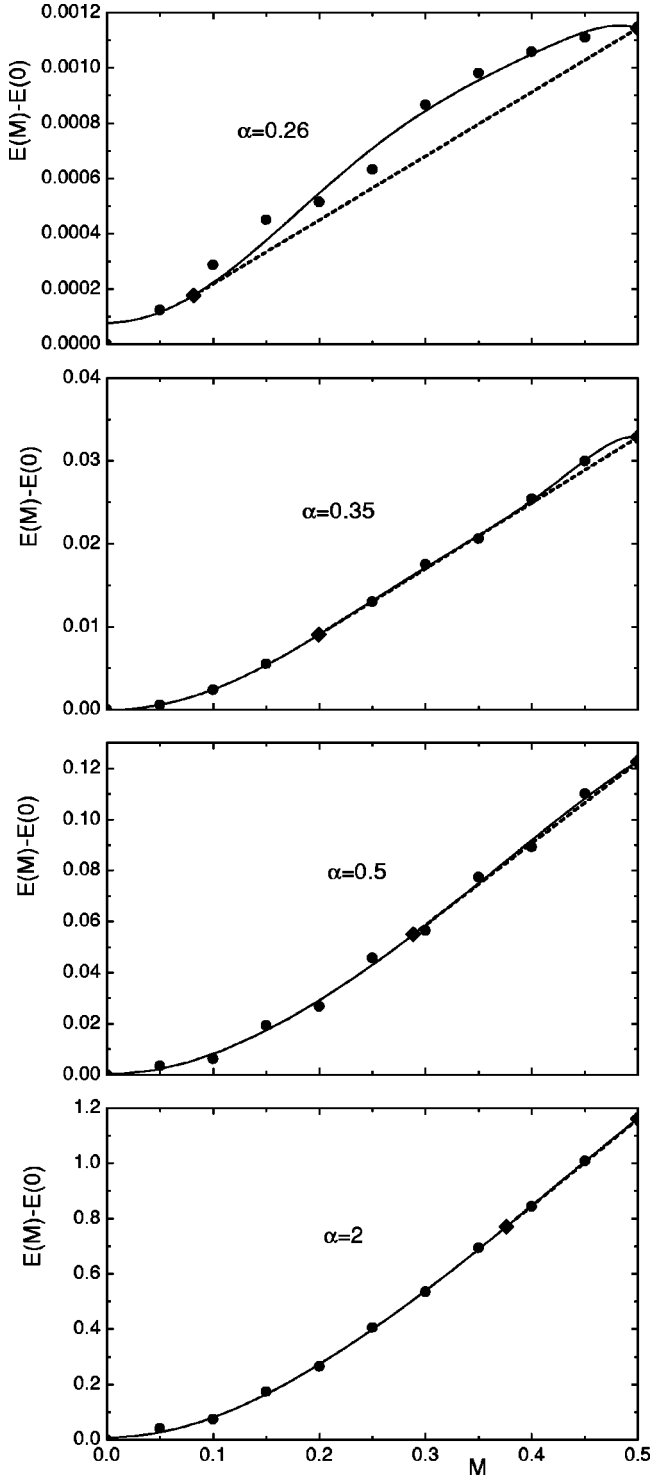

FIG. 4. Energy per site as a function of total spin per site for a chain of 20 sites with $J_1=1$, $\Delta_1=-1$, $\Delta_2=1$, and several values of $\alpha=J_2/J_1$. Full lines are polynomial fits (see the text). Dashed line and diamonds correspond to the Maxwell construction.

the system. To estimate the variation of B_c with α for the isotropic model $\Delta_2=-\Delta_1=1$, we have calculated the average slope of $E(M)$ (minimized with respect to the optimum twisted boundary conditions) between $M=0.3$ and $M=0.5$. The result is shown in Fig. 6. Assuming $g=2$ for the gyro-

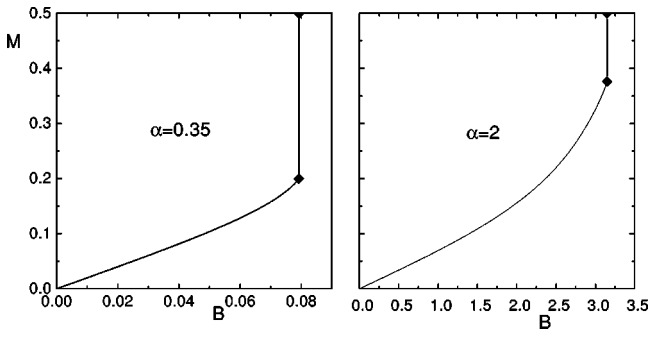

FIG. 5. Total spin per site as a function of magnetic field for $J_1=1$, $\Delta_1=-1$, $\Delta_2=1$, and two values of α.

magnetic factor of the Cu ions, and taking the values of J_1 and α estimated for $La_6Ca_8Cu_{24}O_{41}$, Li_2CuO_2, and $Ca_2Y_2Cu_5O_{10}$,[20] we obtain $B_c=14$, 40, and 65 Tesla, respectively.

V. MAGNETIZATION JUMP IN THE ISOTROPIC CASE

The results of the previous section for $\Delta_2=-\Delta_1=1$, show that there is an abrupt increase in $M(B)$ for $B\sim B_c(\alpha)$ near $M=1/2$, particularly for $1/4<\alpha\leqslant 1/2$. However, they are not enough to establish the existence of a true jump. The calculation of $\partial^2 E/\partial M^2|_{M=1/2}$ becomes complicated by the fact that, independently of system size (at least for $L\lesssim 40$ and near $M=1/2$), only states with total spin $S=L/2-In_{\min}$ with I, $n_{\min}$ integers, but $n_{\min}>1$, can be of thermodynamic relevance. In other words, the curve $E(M)$ near $M=1/2$ looks like a straight line of slope B_c plus a periodic function with period $n_{\min}/L$ (see for example Fig. 4 for $\alpha=0.5$, where $n_{\min}=2$; and Fig. 7 for $\alpha=0.3$, where $n_{\min}=3$). If $\partial^2 E/\partial M^2|_{M=1/2}>0$, this means (as stated in Ref. 8) that reducing the magnetic field from values high enough to ensure saturation of the magnetization, the spins flip in groups of $n_{\min}$. The physical reason of this behavior is not completely clear. It seems that spin flips tend to bind in groups of $n_{\min}$.

As a consequence, Eq. (2), which could be calculated analytically, becomes invalid and should be replaced by

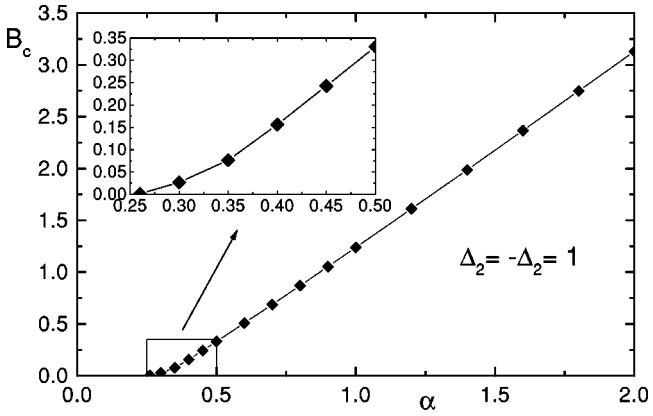

FIG. 6. Critical magnetic field as a function of α for $J_1=1$, $\Delta_1=-1$, and $\Delta_2=1$.

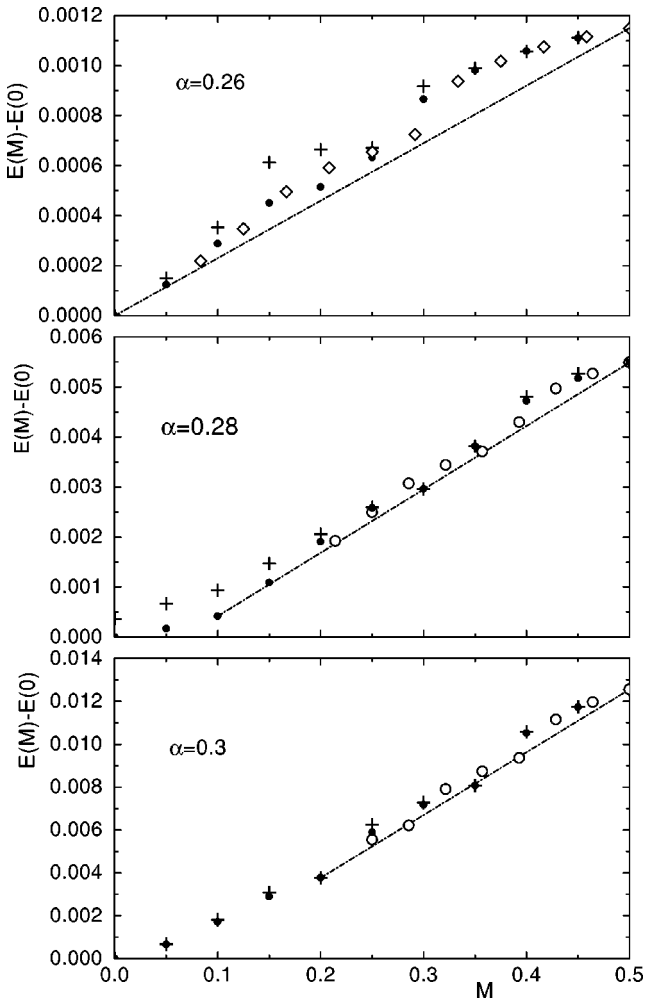

FIG. 7. Energy per site as a function of magnetization for $J_1=\Delta_2=-\Delta_1=1$, and several values of $\alpha=J_2/J_1$ and system sizes: solid circles $L=20$, empty diamonds $L=24$, and empty circles $L=28$. Crosses correspond to $L=20$ using periodic (instead of twisted) boundary conditions. The dot-dashed line joins the points with $M=1/2$ and $M=1/2-2n_{\min}/L$ for $L=20$.

$$\partial^2 E/\partial M^2|_{M=1/2}=\lim_{L\to\infty}\frac{L^2}{n_{\min}^2}[E(1/2)+E(1/2-2n_{\min}/L)-2E(1/2-n_{\min}/L)]. \quad (15)$$

While $n_{\min}=2$ for $\alpha>0.4$, $n_{\min}$ increases with decreasing α, making larger system sizes necessary for an accurate evaluation of Eq. (15). In addition, this equation cannot be used for values of α for which $n_{\min}$ is not well defined. For example $\alpha\sim 0.35$ (see Fig. 4) seems to correspond to a transition from $n_{\min}=2$ to $n_{\min}=3$ with lowering α. Taking into account these difficulties, we have chosen three values of α in the range $1/4<\alpha\leqslant 0.3$, with apparently well-defined values of $n_{\min}$ (3, 4, and 5 for $\alpha=0.3$, 0.28, and 0.26, respectively, see Fig. 7), and have calculated Eq. (15) as a function of system size. For $\alpha=0.3$, for which the energy with six ($2n_{\min}$) spin flips should be calculated, the largest system size considered was $L=40$. This was reduced to $L=28$ and

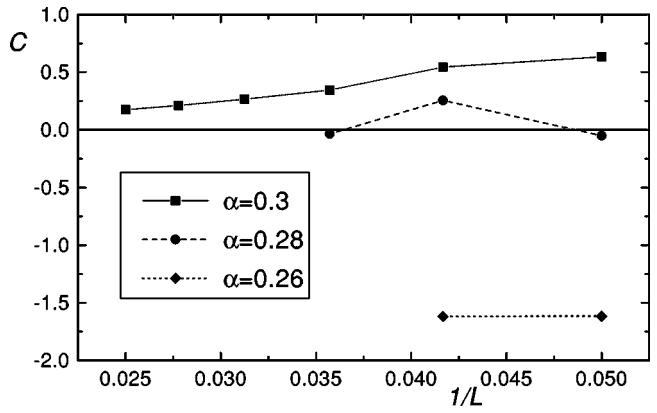

FIG. 8. Relative curvature $C=\partial^2 E/\partial M^2|_{M=1/2}/[E(1/2)-E(0)]$ calculated using Eq. (15) as a function of the inverse of the system size for $J_1=\Delta_2=-\Delta_1=1$, and several values of α.

$L=24$ for $\alpha=0.28$ and 0.26, respectively, due to the increase in $2n_{\min}$. We have taken L multiple of four to avoid frustration of the next-nearest-neighbor antiferromagnetic interaction J_2.

The results of $E(M)$ for two different system sizes and the three values of α are shown in Fig. 7. The oscillations with period $n_{\min}/L$ are clearly seen. We also show a comparison with the result of periodic boundary conditions. As before, the minimization with respect to twisted boundary conditions reduces the magnitude of these oscillations and the finite-size effects, particularly for α near 1/4, small M, and smaller L. With increasing L, the points tend to lie nearer to the dot-dashed line. As mentioned before,[12] for any system size, minimization with respect to twisted boundary conditions reproduces the exact energy and wave vector in the one magnon sector: for $\alpha\geqslant 1/4$ and $M=1/2-1/L$, $q=\pm\arccos[-1/(4\alpha)]$ and

$$E(1/2-1/L)=(\Delta_1+\alpha\Delta_2)J_1/4-[\Delta_1+\alpha(1+\Delta_2)+1/(8\alpha)]/L.$$

However, for $\alpha=0.3$, evaluation of Eq. (15) is not affected by the use of periodic boundary conditions, since they minimize the energy for three and six spin flips. Then, our results for $\alpha=0.3$ are consistent with those of Cabra *et al.*, who using periodic boundary conditions obtain that $M(B)$ is very steep near $M=1/2$, but without a jump for $\alpha=1/3$ (Fig. 4 of Ref. 8).

In Fig. 8, we represent the dimensionless relative curvature:

$$C=\frac{\partial^2 E/\partial M^2|_{M=1/2}}{E(1/2)-E(0)},$$

where the numerator is evaluated using Eq. (15) with different values of L, and in the denominator the result for $L=20$ is taken. Except for the case of $\alpha=0.28$, in which there seems to be an oscillating behavior of C with L, the variation of C with L is rather smooth. For $L=24$ ($1/L\simeq 0.042$) the values of C are shifted upwards with respect to a smooth curve that fits the rest of the points. For $\alpha=0.26$, different extrapolations of the data to the thermodynamic limit give $|C|<0.1$. Since this value is of the order of the uncertainty in the extrapolations, a definite conclusion regarding the sign of C cannot be drawn. Similary, for $\alpha=0.28$, due to the oscillating behavior of the data, no reliable extrapolation can be made. Instead, for $\alpha=0.26$, although we have only two points available, it is remakkable that the curvature is practically constant ($C=-1.617$) suggesting a negative value in the thermodynamic limit. Taking into account that for $\alpha=0.28$ and 0.26, the curvature for $L=24$ seems shifted to higher values in comparison with the rest of the curve, the sign of C for all finite L, and the behavior of $E(M)$ displayed in Fig. 7 for each value of α, we believe that C changes sign for α_c slightly below 0.28. For $0.25<\alpha<\alpha_c$, we expect a true jump in $M(B)$.

VI. SUMMARY AND DISCUSSION

We have investigated by analytical and numerical methods, the regions of parameters Δ_1, Δ_2 and $\alpha=J_2/J_1$ for which a jump in the magnetization as a function of magnetic field $M(B)$, of the spin-1/2 XXZ chain with next-nearest-neighbor exchange [Eq. (1)] is expected. The numerical results are restricted to the region $|\Delta_1|\leqslant 1$ and $0\leqslant\Delta_2\leqslant 1$.We were particularly interested in parameters near the isotropic limit of ferromagnetic J_1 and antiferromagnetic J_2 ($\alpha>0$, $\Delta_2=-\Delta_1=1$), which are relevant to some systems containing CuO chains with edge-sharing CuO_4units.[20]

One of the necessary conditions for a jump in $M(B)$ is that the ground-state energy per site as a function of magnetization $E(M)$ should have zero or negative curvature in a finite interval. In absence of even-odd effects or spin flips in groups as discussed in Secs. IV and V, respectively, the curvature at maximum M ($\partial^2 E/\partial M^2|_{M=1/2}$) can be calculated analytically in the thermodynamic limit from the energy of the states with one and two magnons. The resulting points of zero curvature define a surface S_1 in the parameter space α,Δ_1,Δ_2, which turns out to be a frontier for the occurrence of metamagnetic transitions. The rest of the boundary of the region of expected metamagnetism was constructed from the condition $E(0)=E(1/2)$, where $E(M)$ was calculated numerically in chains of 20 sites. We call this surface S_2.

For $-1\geqslant\Delta_1\geqslant 0$, the line of S_1 given by

$$4\alpha\Delta_1+1=0,\quad 1+\Delta_2-2\Delta_1^2=0$$

on which the wave vector of the two-magnon ground state in the thermodynamic limit changes from $K=0$ to $K=\pm 2\arccos[-1/(4\alpha)]$ *coincides* with a line of S_2 in which $E(M)$ is independent of M. Thisnoticeable property allows to split the regions of expected metamagnetism in two, depending if α is moved to lower or higher values from this line (see Figs. 2 and 3). Inside the first region, the existence of a jump in $M(B)$ is confirmed calculating $E(M)$ numerically, for all possible M in a finite chain. At least for $|\Delta_i|\leqslant 1$, this region disappears if $\Delta_1=-1$ or $\Delta_2=1$. However, particularly for $\alpha=1/4$, there are values of Δ_1 and Δ_2 near

the isotropic case $\Delta_2=-\Delta_1=1$ for which a metamagnetic transition exists. The intersection of S_1 with the plane $\alpha=1/4$ gives the simple equation:

$$2\Delta_1\Delta_2+2\Delta_1+3\Delta_2+1=0.$$

Displacing one of the Δ_i slightly to lower values from this line (without reaching S_2) is enough to have a jump in $M(B)$ (see Fig. 1).

In the second region of expected metamagnetism (larger values of α), the analytical calculation of S_1 becomes invalid due to the tendency of the system to decrease the magnetization from saturation in more than one spin flip. Numerical calculations of the curvature $\partial^2E/\partial M^2$ in the isotropic case $\Delta_2=-\Delta_1=1$ near $M=1/2$, using states with adequately chosen total spin and twisted boundary conditions (which allow for incommensurate wave vectors[12] and are crucial here), suggest that it remains negative for $\alpha<\alpha_c$ with $\alpha_c\sim0.28$ or slightly less. A jump in $M(B)$ exists for $1/4<\alpha<\alpha_c$. In any case, even for $\alpha>\alpha_c$, our results seem enough to show that $M(B)$ should have an abrupt increase (if not a true jump) from nearly 60% to 100% of the magnetization of saturation at a critical field B_c. As an example, taking the parameters of Ref. 20, we estimate $B_c=14$ and 40 Tesla for $La_6Ca_8Cu_{24}O_{41}$ and Li_2CuO_2, respectively.

ACKNOWLEDGMENTS

I am grateful to F. H. L. Eßler, C. D. Batista, D. Cabra, A. Honecker, and Ana López for important discussions. I acknowledge computer time at the Max-Planck Institute für Physik Komplexer Systeme. I was partially supported by CONICET. This work was sponsored by PICT 03-00121-02153 of ANPCyT and PIP 4952/96 of CONICET.

[1] N. Motoyama, H. Eisaki, and S. Uchida, Phys. Rev. Lett. **76**, 3212 (1996).
[2] M. Matsuda, K. Katsumata, K.M. Kojima, M. Larkin, G.M. Luke, J. Merrin, B. Nachumi, Y.J. Uemura, H. Eisaki, N. Motoyama, S. Uchida, and G. Shirane, Phys. Rev. B **55**, R11 953 (1997).
[3] R. Coldea, D.A. Tennant, R.A. Cowley, D.F. McMorrow, B. Dorner, and Z. Tylczynski, Phys. Rev. Lett. **79**, 151 (1997).
[4] D.C. Johnston, M. Troyer, S. Miyahara, D. Lidsky, K. Ueda, M. Azuma, Z. Hiroi, M. Takano, M. Ysobe, Y. Ueda, M.A. Korotin, V.I. Anisimov, A.V. Mahajan, and L.L. Miller, cond-mat/0001147 (unpublished).
[5] R. Bursill, G.A. Gehring, D.J.J. Farnell, J.B. Parkinson, T. Xiang, and C. Zeng, J. Phys.: Condens. Matter **7**, 8605 (1995).
[6] S.R. White and I. Affleck, Phys. Rev. B **54**, 9862 (1996).
[7] A.A. Nersesyan, A.O. Gogolin, and F.H.L. Eßler, Phys. Rev. Lett. **81**, 910 (1998).
[8] D. Cabra, A. Honecker, and P. Pujol, Eur. Phys. J. B **13**, 55 (2000).
[9] C. Gerhardt, K.-H. Mütter, and H. Kröger, Phys. Rev. B **57**, 11 504 (1998).
[10] S. Hirata and K. Nomura, Phys. Rev. B **61**, 9453 (2000).
[11] S. Hirata, cond-mat/9912066 (unpublished).
[12] A.A. Aligia, C.D. Batista, and F.H.L. Eßler, Phys. Rev. B **62**, 3259 (2000).
[13] C. Itoi and S. Qin, cond-mat/0006155 (unpublished).
[14] T. Hikihara, M. Kaburagi, and H. Kawamura, cond-mat/0007095 (unpublished).
[15] H. Bjerrum Møller, S.M. Shapiro, and R.J. Birgeneau, Phys. Rev. Lett. **39**, 1021 (1977).
[16] A. Ito, S. Ebii, H. Aruga Katori, and T. Goto, J. Magn. Magn. Mater. **104-107**, 1635 (1992).
[17] E. Lelièvre-Berna, B. Ouladdiaf, R.M. Galéra, J. Deportes, and R. Ballou, J. Magn. Magn. Mater. **123**, L249 (1993).
[18] D. Eckert, K. Ruck, M. Wolf, G. Krabbes, and K.-H. Müller, J. Appl. Phys. **83**, 7240 (1998).
[19] A.A. Aligia, cond-mat/0006178, J. Magn. Magn. Mater. (to be published).
[20] Y. Mizuno, T. Tohyama, S. Maekawa, T. Osafune, N. Motoyama, H. Eisaki, and S. Uchida, Phys. Rev. B **57**, 5326 (1998).
[21] A.A. Ovchinnikov, Mod. Phys. Lett. B **7**, 21 (1993); A.A. Aligia, L. Arrachea, and E.R. Gagliano, Phys. Rev. B **51**, 13 774 (1995); E.R. Gagliano, A.A. Aligia, L. Arrachea, and M. Avignon, *ibid.* **51**, 14 012 (1995).
[22] I.S. Gradshtein and I.M. Ryzhik, *Tables of Integrals, Series and Products* (Academic Press, New York, 1980), p. 379.
[23] T. Hamada, J. Kane, S. Nakagawa, and Y. Natsume, J. Phys. Soc. Jpn. **57**, 1891 (1988).